

Defect-Structure-Related Ferroelectric Properties of $K_{0.5}Na_{0.5}NbO_3$ Lead-Free Piezoelectric Ceramics

Shanming Ke¹, Manfang Mai¹, Tao Li¹, Mao Ye¹, Peng Lin^{1,*}, Xierong Zeng¹, L.M. Zhou², Y.W. Mai^{2,3} and Haitao Huang^{4,*}

¹College of Materials Science and Engineering and Shenzhen Key Laboratory of Special Functional Materials, Shenzhen University, Shenzhen 518060, China

²Department of Mechanical Engineering, The Hong Kong Polytechnic University, Hong Kong

³Center for Advanced Materials Technology (CAMT), School of Aerospace, Mechanical and Mechatronic Engineering J07, University of Sydney, Sydney, NSW 2006, Australia

⁴Department of Applied Physics and Materials Research Centre, The Hong Kong Polytechnic University, Hong Kong

Abstract: Lead-free piezoelectric ceramics $K_{0.5}Na_{0.5}NbO_3$ (KNN) doped with Cu, Fe, and Ni have been prepared by a conventional ceramic process. The results reveal that Cu-doped KNN ceramic exhibits double-loop-like characteristics, while Fe & Ni-doped KNN ceramics show normal single loops. EPR spectra verified the formation of irreversible defect complex $(Cu_{Nb}^m - V_O^{\bullet\bullet})'$ (DC1) and $(V_O^{\bullet\bullet} - Cu_{Nb}^m - V_O^{\bullet\bullet})^\bullet$ (DC2) in Cu-doped ceramics, while defect complexes were observed in Fe-doped ceramics and very small defect complex signal in Ni-doped ceramics. The experimental results show that the ferroelectric properties of KNN ceramics are strongly related to these defect structures.

Keywords: Defect complex, $K_{0.5}Na_{0.5}NbO_3$, EPR, Ferroelectric polarization, KNN ceramics.

1. INTRODUCTION

As a lead-free ferroelectric, potassium sodium niobate ($K_xNa_{1-x}NbO_3$, KNN) has become an object of intensive research in the past decade [1-3]. The Curie temperature of KNN is comparatively high (about 420°C), which allowing operation in a wide temperature range. However, similar to many other electroceramics, the electric properties of pure KNN are only moderate and then should be improved or tailored for some specific applications. A common strategy for tailoring the properties of electro ceramics is doping on a percentage level. Acceptor dopants in ferroelectric oxides are substitutional cations which can attract oxygen vacancies for charge compensation and thus form defect complexes or defect dipoles. The interaction between these defect complexes with the domain structures has pronounced impact on the hardening, aging, and fatigue behaviors of ferroelectrics [4, 5].

It is generally believed that defect dipoles contribute to ferroelectric hardening by impeding the motion of domain walls. Furthermore, double polarization-electric field (*P-E*) hysteresis loops have been observed in

many acceptor-doped ferroelectrics (FEs), such as Cu-doped KNN ceramics [6-8]. This phenomenon has been explained on the basis of the high mobility of defect dipoles, which could reorient easily after the formation domain patterns during the fabrication process and then could provide the driving force for domain back-switching [1, 6-8]. From our [2] and Eichel *et al* previous study [7, 8], two kinds of defect complexes $(Cu_{Nb}^m - V_O^{\bullet\bullet})'$ (DC1) and $(V_O^{\bullet\bullet} - Cu_{Nb}^m - V_O^{\bullet\bullet})^\bullet$ (DC2) are preferred to form in Cu-doped KNN. The DC1 defect possesses an electric dipole moment and then could provide a driving force, while DC2 has an elastic dipole moment. In respect to the defect structure, it is interesting to investigate the influences of different acceptor dopants on the electric properties of KNN ceramics. In the present work, Cu, Fe and Ni were used as acceptor dopants to modify the ferroelectric properties of KNN ceramics. The corresponding defect structures were characterized by electron paramagnetic resonance (EPR) spectroscopy. Very different defect structures were observed in these material systems with corresponding ferroelectric properties.

2. EXPERIMENTAL

Ceramics with nominal composition $K_{0.5}Na_{0.5}(Nb_{0.996}Cu_{0.01})O_3$ (abbreviated as KNN-Cu), $K_{0.5}Na_{0.5}(Nb_{0.996}Ni_{0.01})O_3$ (KNN-Ni), and

*Address correspondence to this author at the College of Materials Science and Engineering and Shenzhen Key Laboratory of Special Functional Materials, Shenzhen University, Shenzhen 518060, China; Tel: +852 2766 5694; Fax: +852 2333 7629; E-mail: aphhuang@polyu.edu.hk and lin.peng@szu.edu.cn

$K_{0.5}Na_{0.5}(Nb_{0.994}Fe_{0.01})O_3$ (KNN-Fe) were prepared by the conventional solid state reactions. Appropriate quantities of K_2CO_3 (99.9%), Na_2CO_3 (99.9%), Nb_2O_5 (99.99%), CuO (99.8%), Fe_2O_3 (99.9%), and NiO (99.9%) were mixed by ball milling in ethanol and then calcined at $850^\circ C$ for 2.5 h. After calcination, the mixture was ball milled again and then pressed into disks at a cold-isostatic pressure of 300 MPa. The green pellets were sintered at $1070^\circ C$ - $1090^\circ C$ for 4 h in a K/Na rich ambient.

X-ray diffraction (XRD) was conducted on polish surfaces of sintered ceramics at room temperature. Data were collected on an automated diffractometer (Bruker Advanced D8) with $Cu K_{\alpha 1}$ radiation. The fracture surfaces of the ceramic pellets were examined by scanning electron microscopy (Nova Nano SEM450). X-band electron paramagnetic resonance (EPR) spectrum was recorded at 3.8 K with a Bruker EMX EPR spectrometer with standard experimental condition. Top and bottom electrodes were made by coating silver paint on both sides of the sintered and polished disks and followed by firing at $550^\circ C$ for 20 minutes. The dielectric properties were measured as a function of temperature using a LCR meter (HP4194A, CA). The P - E loops were measured by a standard ferroelectric analyzer (TF-2000, Aachen, Germany).

3. RESULTS AND DISCUSSION

Figure 1 shows the XRD patterns of KNN-Cu, KNN-Fe, and KNN-Ni ceramics, respectively. It can be seen that all these samples present a pure perovskite phase with an orthorhombic unit cell at room temperature without a secondary phase, which can be detected within experimental uncertainty. It suggests that Cu^{2+} ,

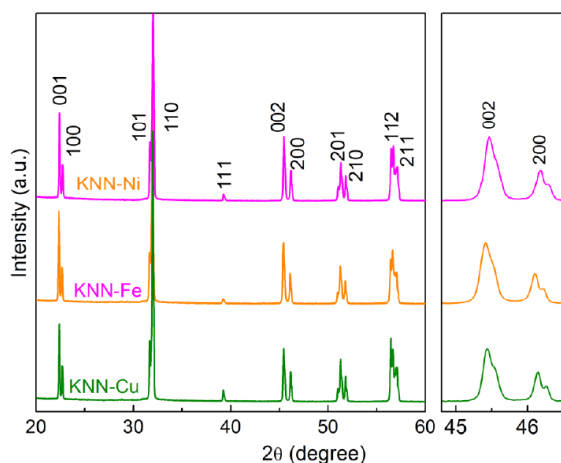


Figure 1: (Color online) XRD patterns of the KNN-Cu, KNN-Fe, and KNN-Ni ceramics.

Fe^{3+} and Ni^{2+} were incorporated into the perovskite structure and the solubility limits are all more than 1%. All the (200) peaks split into two peaks, confirming all the samples have an orthorhombic phase but not monoclinic. The calculated lattice parameters are $a=4.0018\text{\AA}$, $b=4.0129\text{\AA}$, $c=3.9437\text{\AA}$ for KNN-Cu, $a=3.9975\text{\AA}$, $b=4.0065\text{\AA}$, $c=3.9352\text{\AA}$ for KNN-Ni, and $a=3.9951\text{\AA}$, $b=4.0069\text{\AA}$, $c=3.9327\text{\AA}$ for KNN-Fe, respectively. The unit cell becomes smaller with small dopant cations.

The temperature dependence of dielectric constant and dielectric loss of KNN-Cu, KNN-Fe, and KNN-Ni at 1 MHz are shown in Figure 2. Similar to previous reports [9], phase transitions are observed at $419^\circ C$ and $213^\circ C$ for KNN-Cu, which correspond to the cubic-to-tetragonal (T_{C-T}) and tetragonal-to-orthorhombic (T_{T-O}) transitions, respectively. The Fe- and Ni-substituted KNN ceramics exhibit very similar dielectric peaks with nearly same phase transition temperatures. Both the phase transitions T_{C-T} and T_{T-O} of these samples decreased $3^\circ C$ and $13^\circ C$ comparing with pure KNN [10]. It is clear that the peaks of all samples at the Currie temperature are sharp indicating that the ceramics show a normal ferroelectric behavior. Two broad dielectric loss peaks could be observed in Figure 2(b) for KNNFe, which have been often found in KNN-

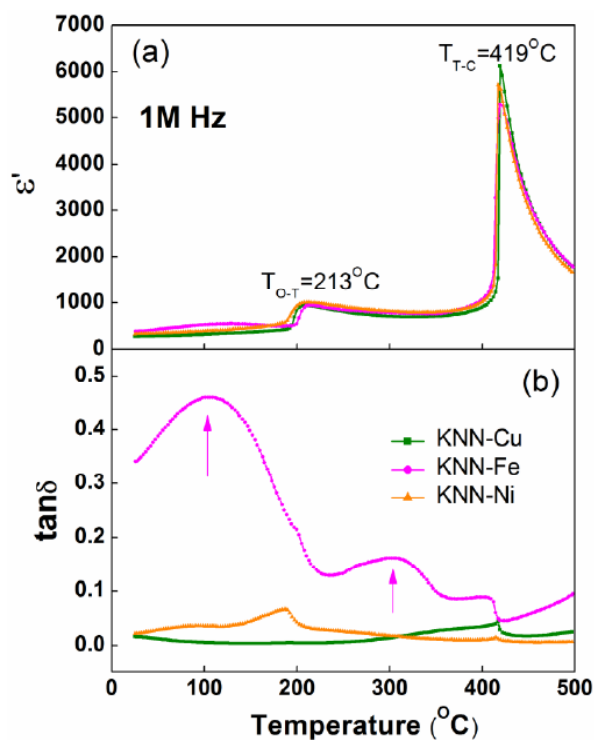


Figure 2: (Color online) Temperature dependence of dielectric constant and dielectric loss at 1 MHz for the KNN-Cu, KNN-Fe, and KNN-Ni ceramics.

based ceramics [11] and were generally attributed to the migration of vacancy defects.

Figure 3 shows the room temperature P - E loops at 1 Hz for the KNN-Cu, KNN-Fe, and KNN-Ni ceramics, respectively. Similar to earlier reports [2, 6], KNN-Cu display a double hysteresis loop. It has been proposed that the defect complex DC1 is responsible for the double P - E loop in KNN-Cu [2, 6]. Non-switchable DCs that are aligned opposite to the spontaneous polarization (P_s) direction provide the driving force for domain back-switching after the removal of the external electric field, similar to the antiferroelectric behavior. Considering the similar acceptor doping nature, it would be expected that Ni and Fe dopants should create similar double P - E loops. However, only a typical ferroelectric single loop can be observed in the KNN-Ni and KNN-Fe ceramics, with remnant polarization (P_r) of 25.3 and 42.4 $\mu\text{C}/\text{cm}^2$, respectively.

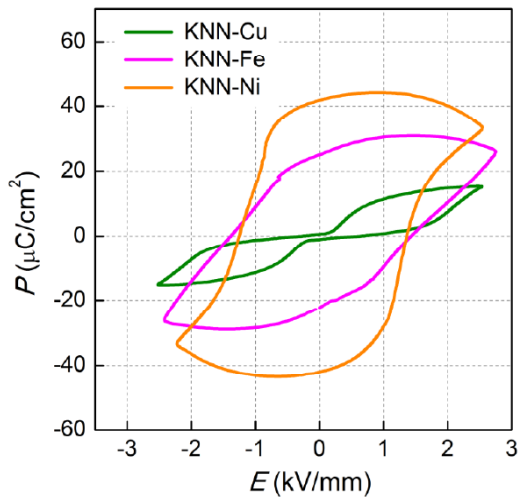
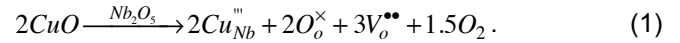
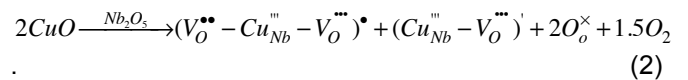


Figure 3: (Color online) P - E loops of the KNN-Cu, KNN-Fe, and KNN-Ni ceramics at 1 Hz.

First-principles calculations [12] have revealed that the most stable configuration for Cu-doped KNN in thermal equilibrium at room temperature is the substitution on Nb sites. While Cu atoms substitute Nb atoms, oxygen vacancies are formed as a charge compensation mechanism. The incorporation reaction can be given as



In this case, there are 1.5 oxygen vacancies per Cu center. EPR (Figure 4a) shows that the Cu is prefer to form dimeric (DC1) and trimeric (DC2) complexes [2-4], and then the result of doping with CuO can be written as



Schematically, the defect complex configurations of DC1 and DC2 are illustrated in Figure 5. It is clearly seen that DC1 contains an electric dipole moment (P_D), while the dipole moment for DC2 almost vanishes due to its symmetric configuration. Because of its non-dipolar nature, DC2 cannot induce the double P - E loops.

For KNN-Fe compounds, it can be expected that the Fe^{3+} center acts as an acceptor and forms $(\text{Fe}_{\text{Nb}}^{\text{III}} - \text{V}_o^{\bullet\bullet})$ defect for charge compensation [13]. It may be a $(\text{Fe}_{\text{Nb}}^{\text{III}} - \text{V}_o^{\bullet\bullet})_{\parallel}$ defect dipole oriented along the direction of spontaneous polarization, or a $(\text{Fe}_{\text{Nb}}^{\text{III}} - \text{V}_o^{\bullet\bullet})_{\perp}$ defect dipole oriented perpendicular to the orientation of spontaneous polarization. In EPR spectra, the resonance at 110 mT represents the existence of $(\text{Fe}_{\text{Nb}}^{\text{III}} - \text{V}_o^{\bullet\bullet})_{\parallel}$, while the resonance at around 151 mT

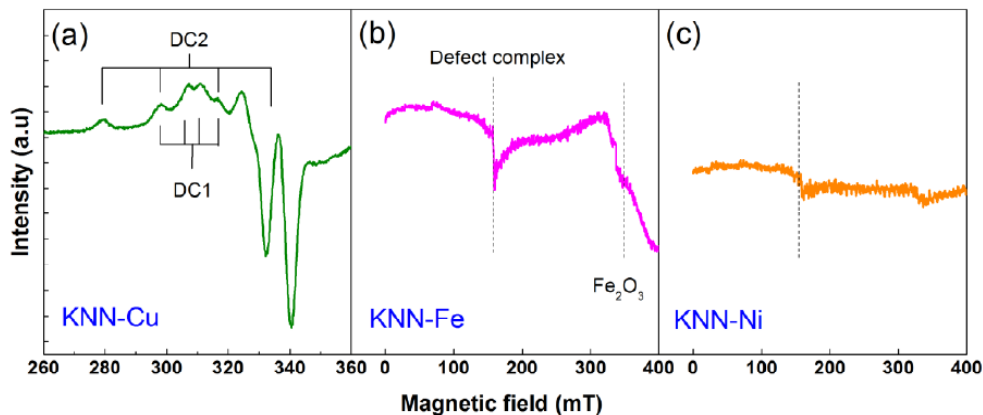


Figure 4: (Color online) X-Band (9.4 GHz) EPR-spectra of the KNN-Cu, KNN-Fe, and KNN-Ni ceramics at 3.8 K. DC1 denotes the $(\text{Cu}_{\text{Nb}}^{\text{III}} - \text{V}_o^{\bullet\bullet})^{\prime}$ and DC2 denotes the $(\text{V}_o^{\bullet\bullet} - \text{Cu}_{\text{Nb}}^{\text{III}} - \text{V}_o^{\bullet\bullet})^{\bullet}$ defect complexes. The defect complex in KNN-Fe reveals dimer $(\text{Fe}_{\text{Nb}}^{\text{III}} - \text{V}_o^{\bullet\bullet})_{\perp}$.

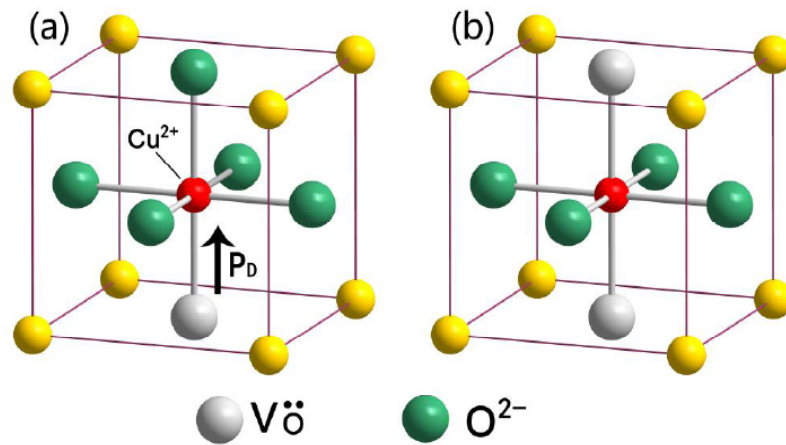


Figure 5: (Color online) Schematic representation of the defect structure in KNN-Cu: (a) $(Cu_{Nb}''' - V_O''')'$ and $(V_O'' - Cu_{Nb}''' - V_O''')^*$. P_D is the polarization associated with the defect complex.

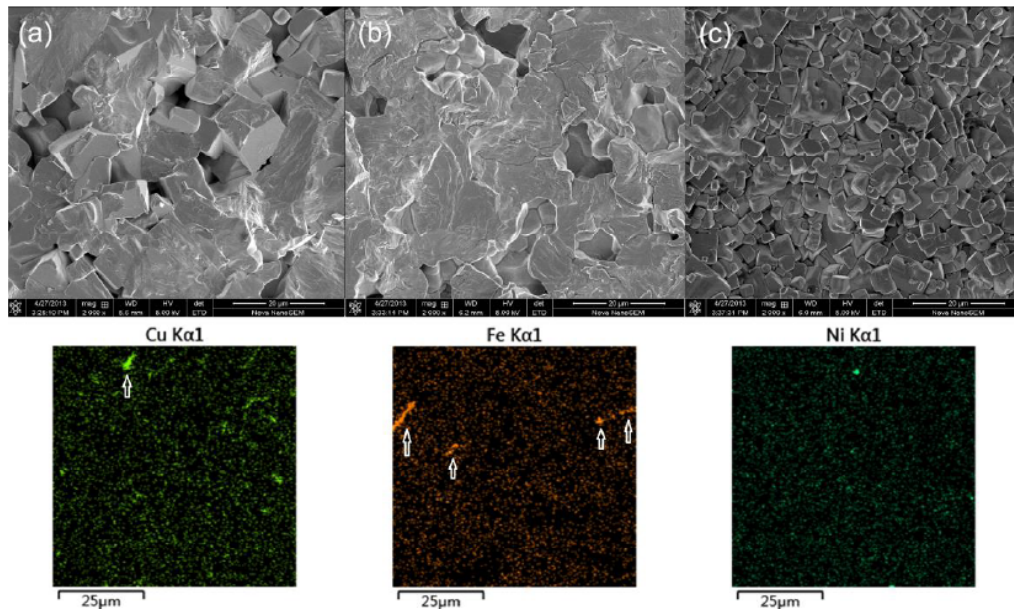


Figure 6: (Color online) SEM images of the fractures of the KNN-Cu, KNN-Fe, and KNN-Ni ceramics with Cu, Fe, and Ni elements mapping.

indicates the existence of $(Fe_{Nb}'' - V_O'')$ defect dipoles [14]. The EPR result of KNN-Fe (as shown in Figure 4b) reveals that only pronounced $(Fe_{Nb}'' - V_O'')$ defects can be observed in our samples. Although $(Fe_{Nb}'' - V_O'')$ contains an electric dipole moment, the perpendicular nature implies it cannot provide enough force for domain switching and then only single $P-E$ loop could be obtained. Due to the similar chemical properties of Cu and Ni ions, the defect structure of KNN-Ni compounds should be very similar to that of KNN-Cu. However, there is very small resonance signals at around 140 mT could be observed in Figure 4c, which means a few Ni-based defect complexes have been produced in KNN-Ni. From the $P-E$ loop

result of KNN-Ni shown in Figure 3, it would simply conclude that the existence of Ni-based defect complexes has very little effect on the polarization of KNN-Ni.

Figure 6 reveals the fracture morphologies of the KNN-Cu, KNN-Fe, and KNN-Ni ceramics. It is clear that KNN-Cu and KNN-Fe display much larger grain size than KNN-Ni samples. The elemental mapping images show clearly that Cu and Ni have a uniform distribution in these ceramics, while Fe-rich phase (as shown in Figure 6) is observed in KNN-Fe samples. These Fe-rich phases could also be detected by the EPR spectra (Figure 4b) and be known as Fe_2O_3 [14]. It is worth

noting that the amount of these secondary phases is too small to be revealed by XRD results.

4. CONCLUSIONS

$K_{0.5}Na_{0.5}(Nb_{0.996}Cu_{0.01})O_3$, $K_{0.5}Na_{0.5}(Nb_{0.996}Ni_{0.01})O_3$, and $K_{0.5}Na_{0.5}(Nb_{0.994}Fe_{0.01})O_3$ lead-free ceramics have been prepared by a conventional ceramic process. All the ceramics possess a perovskite structure with orthorhombic symmetry. The dopants give rise to very different defect configurations and the ferroelectric properties of KNN ceramics are strongly related to these defect structures. EPR spectra verified the formation of irreversible defect complex $(Cu_{Nb}^{III} - V_O^{III})'$ (DC1) and $(V_O^{II} - Cu_{Nb}^{III} - V_O^{III})^*$ (DC2) in Cu-doped ceramics, DC1 of these defects could provide restoring forces to reverse the switched polarizations and thus producing a double $P-E$ loop. $(Fe_{Nb}^{II} - V_O^{II})_{\perp}$ defect complex was observed in Fe-doped ceramics and its perpendicular nature implies it cannot provide enough force for domain switching and only single $P-E$ loop could be obtained. There is no defect complex could be observed in Ni-doped ceramics.

ACKNOWLEDGEMENTS

This work was supported by the National Natural Science Foundations of China (Nos. 51302172 and 51272161) and the Science and Technology Research Items of Shenzhen (No. JCYJ20140509172719306).

REFERENCES

- [1] Saito Y, Takao H, Tani T, Nonoyama T, Takatori K, Homma T, *et al.* Lead-free piezoceramics, *Nature* 432 (2004) 84. <http://dx.doi.org/10.1038/nature03028>
- [2] Ke S, Huang H, Fan H, Lee HK, Zhou L, Mai YW, Antiferroelectric-like properties and enhanced polarization of Cu-doped $K_{0.5}Na_{0.5}NbO_3$ piezoelectric ceramics, *Appl Phys Lett* 101(2012) 082901. <http://dx.doi.org/10.1063/1.4747212>
- [3] Tan X, Fan H, Ke S, Zhou L, Mai YW, Huang H, Structural dependence of piezoelectric, dielectric and ferroelectric properties of $K_{0.5}Na_{0.5}(Nb_{1-2x/5}Cu_x)O_3$ lead-free ceramics with high Q_m , *Mater Res Bull* 47, (2012) 4472. <http://dx.doi.org/10.1016/j.materresbull.2012.09.049>
- [4] Eichel RA, Erüna E, Jakes P, Körbel S, Elsässer C, Kungl H, *et al.* Interactions of defect complexes and domain walls in CuO-doped ferroelectric $K_{0.5}Na_{0.5}NbO_3$, *Appl. Phys. Lett.* 102(2013) 242908. <http://dx.doi.org/10.1063/1.4811268>
- [5] Feng Z, Or SW, Aging-induced, defect-mediated double ferroelectric hysteresis loops and large recoverable electrostrain in Mn-doped orthorhombic $KNbO_3$ -based ceramics, *J Alloys Comp* 480 (2009) L29. <http://dx.doi.org/10.1016/j.jallcom.2009.02.043>
- [6] Lin DM, Kwok KW, Chan HLW, Double hysteresis loop in Cu-doped $K_{0.5}Na_{0.5}NbO_3$ lead-free piezoelectric ceramics, *Appl Phys Lett* 90 (2007) 232903. <http://dx.doi.org/10.1063/1.2746087>
- [7] Eichel RA, Erüna E, Drahus MD, Smyth DM, Tol JV, Acker J, *et al.* Local variations in defect polarization and covalent bonding in ferroelectric Cu^{2+} -doped PZT and KNN functional ceramics at the morphotropic phase boundary, *Phys Chem Chem Phys* 11 (2009) 8698. <http://dx.doi.org/10.1039/b905642d>
- [8] Eichel RA. Structural and dynamic properties of oxygen vacancies in perovskite oxides-analysis of defect chemistry by modern multi-frequency and pulsed EPR techniques, *Phys Chem Chem Phys* 13 (2011) 368. <http://dx.doi.org/10.1039/B918782K>
- [9] Li T, Fan H, Long C, Dong G, Sun S, Defect dipoles and electrical properties of magnesium B-site substituted sodium potassium niobates, *J Alloys Comp* 609 (2014) 60. <http://dx.doi.org/10.1016/j.jallcom.2014.04.024>
- [10] Zuo R, Ma B, Liu Y, Xu Z. Hardening characteristics and compositional dependence of piezoelectric properties in Cu^{2+} modified $0.52NaNbO_3-(0.48-x)KNbO_3-xLiNbO_3$ ceramics, *J Alloys Comp* 488(2009) 465. <http://dx.doi.org/10.1016/j.jallcom.2009.09.012>
- [11] Jiao G, Fan H, Liu L, Wang W. Structure and piezoelectric properties of Cu-doped potassium sodium tantalate niobate ceramics, *Mater Lett* 61(2007) 4185. <http://dx.doi.org/10.1016/j.matlet.2007.01.051>
- [12] Körbel S, Elsässer C. Alignment of ferroelectric polarization and defect complexes in copper-doped potassium niobate *Phys Rev B* 88 (2013) 214114. <http://dx.doi.org/10.1103/PhysRevB.88.214114>
- [13] Erüna E, Eichel RA, Körbel S, Elsässer C, Acker J, Kungl H, *et al.* Defect structure of copper doped potassium niobate ceramics, *Funct Mater Lett* 3(2010) 19. <http://dx.doi.org/10.1142/S1793604710000932>
- [14] Erdem E, Jakes P, Parashar S, Kiraz K, Somer M, Rüdiger A, *et al.* Defect structure in aliovalently-doped and isovalently-substituted $PbTiO_3$ nano-powders, *J Phys: Condens Matter* 22 (2010) 345901. <http://dx.doi.org/10.1088/0953-8984/22/34/345901>
- [15]